ELSEVIER

Journal of Nuclear Materials 258–263 (1998) 1414–1419

journal of nuclear materials

Temperature dependence of the radiation damage microstructure in V–4Cr–4Ti neutron irradiated to low dose

P.M. Rice, S.J. Zinkle *

Oak Ridge National Laboratory, Metals and Ceramics Division, P.O. Box 2008, Oak Ridge, TN 37831-6376, USA

Abstract

Transmission electron microscopy (TEM) was performed on a V–4Cr–4Ti alloy irradiated to damage levels of 0.1–0.5 displacements per atom (dpa) at 110–505°C. A high density of small faulted dislocation loops were observed at irradiation temperatures below 275°C. These dislocation loops became unfaulted at temperatures above ~275°C, and a high density of small Ti-rich defect clusters lying on {0 0 1} planes appeared along with the unfaulted loops at temperatures above 300°C. Based on the TEM and tensile measurements, the dislocation barrier strengths of the faulted dislocation loops and {0 0 1} defect clusters are ~0.4–0.5 and 0.25, respectively. This indicates that both types of defects can be easily sheared by dislocations during deformation. Cleared dislocation channels were observed following tensile deformation in a specimen irradiated at 268°C.

1. Introduction

Vanadium alloys with 4–5% Cr and 4–5% Ti have been identified as promising materials for the first wall and blanket structure of fusion reactors [1]. Fast reactor irradiation studies at temperatures of 425–600°C have reported good resistance of these alloys to void swelling and embrittlement. On the other hand, several recent studies in mixed spectrum and fast reactors at 100–400°C have reported significant radiation hardening and embrittlement even at relatively low doses of 0.1–5 displacements per atom (dpa) [2–6]. Relatively little information is known about the microstructure of V–(4–5%)Cr–(4–5%)Ti alloys irradiated at temperatures below 420°C [7–11]. The present paper summarizes some of the key findings of a study of the microstructure of V–4Cr–4Ti following neutron irradiation to 0.1–0.5 dpa at 100–500°C. Further details on the microstructure [12] and mechanical properties [4] of these specimens are given elsewhere.

2. Experimental procedure

Miniature Charpy vee-notch (CVN) and sheet tensile specimens were machined from the US fusion program heat [13] of V–4Cr–4Ti (Wah Chang Albany heat #832665) which contained ~300 ppm O, 85 ppm N and 80 ppm C. The machined specimens were annealed in vacuum ($<10^{-7}$ torr) for 2 h at 1000°C. The grain size after annealing was ~16 μm.

A series of four irradiation capsules, each containing 4–6 subcapsules with different gas gap dimensions to achieve irradiation temperatures of 110–505°C, were utilized in this experiment. The capsules were successively purged with high-purity helium and evacuated with a turbomolecular pump for three cycles prior to irradiation, and then backfilled with He to 10^5 Pa. The irradiation temperature in each subcapsule was continuously monitored by thermocouples that were embedded in the ends of CVN specimens. Three of the capsules were irradiated for 510–540 h to fast ($E > 0.1$ MeV) and thermal ($E < 0.5$ eV) neutron fluences of $\sim 5 \times 10^{24}$ n/m^2 and 2.3×10^{24} n/m^2, respectively, in the V15 or V16 core thimble positions of the High Flux Beam Reactor (HFBR) at Brookhaven National Laboratory. This produced a calculated Cr transmutation level of ~0.1% and a damage level of ~0.5 dpa. The fourth capsule was irradiated to a fast neutron fluence of 1.0×10^{24} n/m^2 (~0.1 dpa). Table 1 summarizes the irradiation conditions for the different subcapsules. Further details on the specimen preparation and irradiation are given elsewhere [2,4].

* Corresponding author. Tel.: +1 423 5767220; fax: +1 423 574064; e-mail: zinklesj@ornl.gov.

0022-3115/98/$19.00 © 1998 Published by Elsevier Science B.V. All rights reserved.
PII: S 0 0 2 2 - 3 1 1 5 (9 8) 0 0 2 0 8 - 6

Table 1
Summary of irradiation conditions for the V–4Cr–4Ti specimens

Dose (dpa)	Irradiation temperature (°C)										
0.1	105				256			295		390	505
0.5	110	160	205	235	260	268	275	307	324	415	

After the irradiated specimens had been mechanically tested, transmission electron microscopy (TEM) specimens were prepared by cutting 0.25 mm wafers from the ends of the CVN specimens and punching 3 mm disks. Some TEM specimens were also prepared from 0.25 mm sheets which were placed in the final two capsules of the irradiation campaign (275–415°C, 0.5 dpa and 110–505°C, 0.1 dpa). The TEM specimens were electropolished with a sulfuric acid and methanol electrolyte cooled to −10°C at a current of 100 mA. The microstructure was examined using Philips CM12 and CM30 electron microscopes operating at voltages of 120 and 300 keV, respectively. Additional diffraction contrast analysis and analytical electron microscopy (AEM) was performed with a Philips CM200 field emission gun microscope at accelerating voltages of 200 kV. Both energy dispersive X-ray spectroscopy (using the scanning TEM mode) and parallel electron energy loss spectroscopy were utilized.

3. Results

The unirradiated microstructure consisted of a solid solution matrix of equiaxed grains. The grain interior contained a low density of titanium oxycarbonitride precipitates which were preferentially located in precipitate bands with a typical interband spacing of ~10 μm. A slight Ti enrichment relative to the matrix was observed at the grain boundaries of the annealed specimens.

The microstructure of the irradiated specimens could be separated into three temperature-dependent categories. In the low temperature regime (<275°C), the microstructure consisted of a high density of small dislocation loops with $a/2\langle 1\,1\,0\rangle$ Burgers vectors. The dislocation loop density was $\sim 1.0\times 10^{23}/m^3$ and the average loop diameter was ~3.0 nm after 0.5 dpa at temperatures between 110°C and 275°C. Fig. 1 shows the typical microstructure for specimens irradiated in this temperature range. There was no measurable (>5 nm) denuded zone for dislocation loops adjacent to grain boundaries in specimens irradiated at 110–275°C.

In the intermediate temperature regime (275–415°C), pronounced temperature-dependent changes in the defect microstructure occurred. Fig. 2 shows the microstructure for an irradiation temperature of 390°C. The Burgers vectors of the dislocation loops changed from ~95% $a/2\langle 1\,1\,0\rangle$ and ~5% $a/2\langle 1\,1\,1\rangle$ at 275°C to ~10% $a/2\langle 1\,1\,0\rangle$ and ~90% $a/2\langle 1\,1\,1\rangle$ at 315°C for a constant dose of 0.5 dpa. The loop diameter and density at 0.5 dpa ranged from 3.7 nm and $1\times 10^{23}/m^3$ at 275°C to 200 nm and $< 10^{20}/m^3$ at 415°C. Loop denuded zones were observed adjacent to grain boundaries, ranging from 40 nm at 295°C (0.1 dpa) to 200 nm at 390°C (0.1 dpa) and 250 nm at 415°C (0.5 dpa). AEM analysis of the grain boundaries indicated oxygen enrichment after 0.5 dpa at 315°C (with no Cr or Ti enrichment) and Cr enrichment after 0.5 dpa at 415°C. A second population of defect clusters lying on {0 0 1} habit planes became visible for irradiation temperatures ⩾ 315°C (Fig. 2), and these defect clusters coarsened with increasing irradiation temperature. The average diameter and density of these {0 0 1} defect clusters

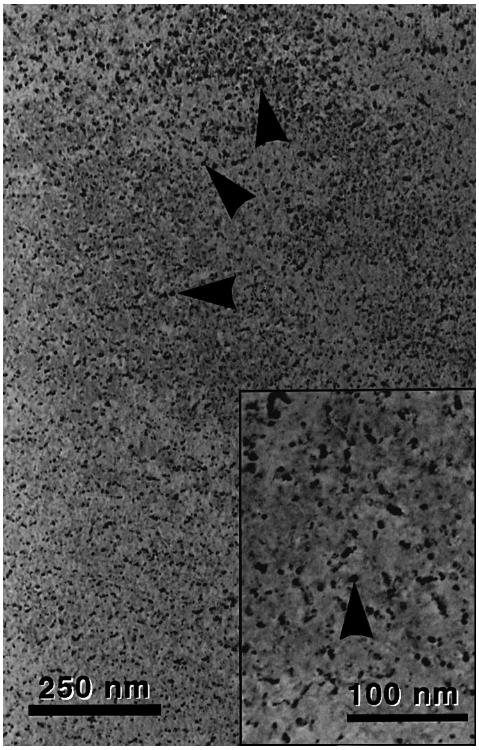

Fig. 1. Dislocation loops in V–4Cr–4Ti irradiated to 0.5 dpa at 110°C. The inset figure shows the loops at a higher magnification. The arrows point to representative loops. The beam direction was 110 and the diffraction vector was $g = 3\bar{3}0$.

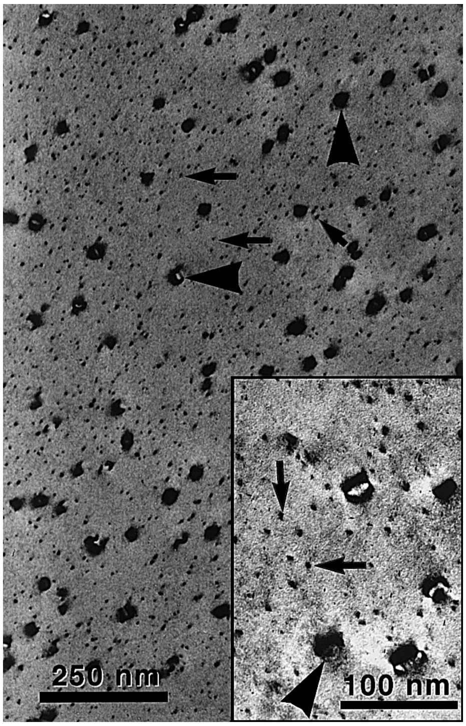

Fig. 2. Microstructure of V–4Cr–4Ti irradiated to a dose of 0.1 dpa at 390°C. The large arrows point to dislocation loops and the small arrows point to several {0 0 1} defect clusters. The inset figure shows the microstructure at a higher magnification. The beam direction was 001 and the diffraction vectors were $g = 200$ ($s_g \sim 0$) and $g = 110$ ($s_g < 0$) for the main and inset photos, respectively.

ranged from <3 nm and > 1.5x10^{23}/m^3 at 315°C to ~40 nm and ~10^{22}/m^3 at 415°C for a constant dose of 0.5 dpa. The {0 0 1} defect clusters appeared to preferentially nucleate adjacent to the dislocation loops, and the {0 0 1} defect distribution was rather inhomogeneous at temperatures ⩾ 415°C due to the low density of dislocation loops. The displacement vector of the {0 0 1} defect clusters was $a/x \langle 0\ 0\ 1 \rangle$ ($x > 1$) at temperatures ⩾ 390°C. Significant segregation of Ti and Cr to the {0 0 1} defects was detected in the 415°C, 0.5 dpa specimen. These two observations indicate that the {0 0 1} defects are precipitates in their early stage of formation. There was no evidence for a denuded zone next to grain boundaries for these defects at irradiation temperatures up to 415°C.

The microstructure in the high temperature regime (>415°C) was dominated by the {0 0 1} defect clusters. Fig. 3 shows the microstructure for V–4Cr–4Ti irradiated to 0.1 dpa at 505°C. A denuded zone width of ~100 nm adjacent to grain boundaries was observed for the {0 0 1} defect clusters. The {0 0 1} defect cluster diameter and density were 42 nm and 2.6×10^{21}/m^3, respectively for this irradiation condition. The corresponding $a/2 \langle 1\ 1\ 1 \rangle$ dislocation loop parameters were 500 nm and <10^{19}/m^3. Significant Ti segregation (but no Cr or O enrichment) with a ~1 nm full-width at half-maximum profile was observed at the {0 0 1} defect clusters at 505°C. The displacement vector of the {0 0 1} defect clusters after 0.1 dpa at 505°C was $a/3 \langle 0\ 0\ 1 \rangle$, again suggesting that these defects are precipitates as opposed to a matrix-based point defect cluster.

Tensile tests performed on specimens irradiated in the same subcapsules [4] found significant radiation hardening at 0.1 and 0.5 dpa for temperatures ⩽ 415°C, with the most pronounced hardening occurring at temperatures ⩽ 315°C (there were no subcapsules at irradiation temperatures between 315°C and 390°C, cf. Table 1). The accompanying decrease in strain hardening capacity at irradiation temperatures ⩽ 315°C resulted in uniform elongations of <0.2% in the tensile specimens [4]. In order to investigate the cause of this plastic instability, TEM specimens were prepared from the deformed gage region of several of the irradiated tensile specimens. Fig. 4 shows an example of the microstructure of the deformed gage region of a tensile specimen irradiated to 0.5 dpa at 268°C. In addition to

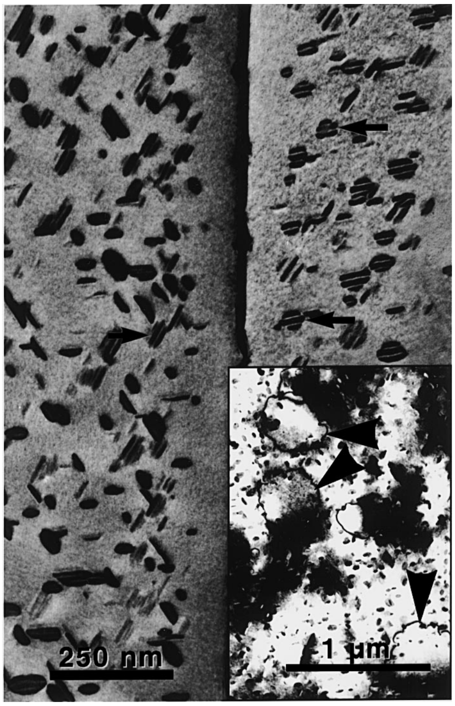

Fig. 3. Microstructure of V–4Cr–4Ti irradiated to a dose of 0.1 dpa at 505°C. The small arrows in the main figure point to several {0 0 1} defect clusters located next to a grain boundary. The large arrows in the inset figure point to several large perfect dislocation loops. The beam direction was 111 and the diffraction vector was $g = 01\bar{1}$.

the high density of small dislocation loops that were present in a nondeformed specimen irradiated at these conditions, cleared dislocation channels on {1 1 0} slip planes were observed. The typical cleared channel width was ~50 nm. Further analysis is needed to determine if some dislocation channels on {2 1 1} slip planes are also present.

4. Discussion

Pronounced radiation-induced microstructural changes occurred in the V–4Cr–4Ti alloy over the entire investigated temperature range of 110–505°C, even at damage levels of 0.1 dpa. The dominant defect at low temperatures ($\leqslant$275°C) was a faulted dislocation loop. Although the nature of the loops was not determined in the present study, previous work on ion-and neutron-irradiated vanadium in this temperature range found that ~80% or more of the dislocation loops in bulk irradiated specimens were interstitial-type [14–17]. The observation of faulted dislocation loops ($b = a/2\langle 1\ 1\ 0\rangle$) in the present study is somewhat surprising, considering the high {1 1 0} stacking fault energy for vanadium. Previous studies have reported $a/2\langle 1\ 1\ 1\rangle$ interstitial dislocation loops for pure vanadium irradiated at low doses (~10^{-4} to 10^{-2} dpa) with protons or 14 MeV neutrons at temperatures between 60°C and 290°C [15,16]. However, their loop analysis at 60–160°C was apparently only performed on relatively large (5–30 nm) loops, many of which formed in the vicinity of network dislocations [15,17]. It is well known [18,19] that dislocation loop unfaulting has a large activation energy barrier. In many cases, loop unfaulting is initiated by the impingement of neighboring loops or network dislocations and cannot be correlated with stacking fault energy. Using similar reasoning, the present observation of metastable faulted dislocation loops in V–4Cr–4Ti up to ~275°C is attributed to the requirement for a high amount of thermal energy to nucleate the unfaulting partial dislocation in the absence of loop impingement processes.

By invoking the simple approximation for dislocation line tension ($T = \mu b^2/2$), the present microstructural data can be combined with sibling tensile data summarized elsewhere [2,4,8] to provide an estimate of the dislocation loop barrier strength (α) using the well-known dispersed barrier hardening equation [20],

$$\Delta\sigma_y = M\alpha\mu b\sqrt{Nd}, \quad (1)$$

where $\Delta\sigma_y$ is the increase in yield strength compared to the unirradiated value, μ is the shear modulus (46 GPa), b is the magnitude of the $a/2\langle 1\ 1\ 1\rangle$ Burgers vector of the dislocations participating in the deformation process

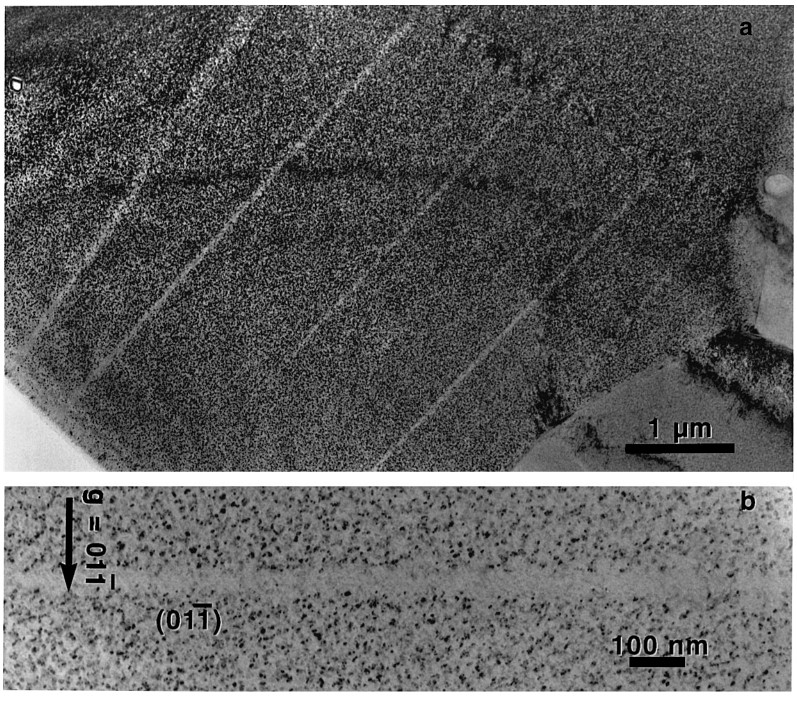

Fig. 4. Cleared dislocation channels in V–4Cr–4Ti irradiated to 0.5 dpa at 268°C and tensile tested at 20°C at a strain rate of 2×10^{-3}/s. Photos (a) and (b) show cleared channels at low and medium magnification, respectively. The beam direction was 111 and the diffraction vector was $g = 01\overline{1}$ in both photos.

(0.262 nm), and N and d are the density and size of the defect clusters. This relation uses the well-known Taylor factor, which has a value of $M = 3.0$ for nontextured FCC and BCC polycrystals [21], to convert the critical resolved shear stress into the polycrystalline yield stress. Many previous radiation hardening studies have used incorrect values of $\sqrt{3}$ or 2 to convert shear stress to polycrystalline yield stress. The calculated value of the barrier strength for the faulted dislocation loops ranges from $\alpha \sim 0.40$–0.50 at irradiation temperatures of 110°C and 200–275°C, respectively. This value is considered to be an upper limit since defect clusters below ~1.5 nm were not resolvable in the TEM specimens. Previous work on low temperature ($\leqslant$ 200°C) neutron-irradiated pure vanadium generally gives similar values of $\alpha \sim 0.18$–0.36 [22–26], where the originally published data in Refs. [22–25] have been revised using the correct value for the Taylor factor ($M = 3.0$). A somewhat higher value of $\alpha \sim 0.75$ (revised using $M = 3.0$) was obtained in another low temperature study of neutron-irradiated pure vanadium [27].

The value of the barrier strength in the V–4Cr–4Ti specimens irradiated at low temperatures is much less than the Orowan value for impenetrable obstacles of $\alpha = 1$ (or $\alpha = 0.8$ for randomly distributed obstacles). Therefore, these small dislocation loops can be sheared or otherwise bypassed during deformation, as evidenced by the cleared dislocation channels in the deformed gage region of V–4Cr–4Ti tensile specimens irradiated at temperatures below 315°C (Fig. 4). The presence of cleared dislocation channels is a well-known phenomenon in numerous FCC and BCC metals irradiated at low temperatures, and is the cause of the pronounced loss of strain hardening capacity (low uniform elongation) in the engineering stress-strain curves [28]. Several previous studies have reported dislocation channeling in vanadium irradiated at temperatures below ~200°C [22,29]. Although flow localization was not detected in the V–4Cr–4Ti tensile specimens irradiated at 390–415°C to 0.1–0.5 dpa in the present study, the TEM and tensile [4] data yield a calculated defect cluster barrier strength of $\alpha = 0.25$ (primarily due to the small {0 0 1} defects). This suggests that cleared dislocation channels and low strain hardening capacity may occur at higher doses (when the cluster density exceeds a critical value), unless the {0 0 1} cluster size increases and becomes an Orowan obstacle at higher doses. Dislocation channeling has been recently observed in the deformed gage regions of V–4Cr–4Ti specimens that were irradiated to 4 dpa at 400°C [30].

In contrast to the temperature-independent microstructure which occurred below 275°C, pronounced temperature-dependent microstructural changes occurred above 275°C. The total defect cluster density remained nearly constant for irradiation temperatures approaching 400°C, since the unfaulting and coarsening of the dislocation loops was partially balanced by the appearance of a high density of defect clusters on {0 0 1} habit planes whose density decreased slowly with increasing temperature between 315°C and 390°C. The enriched Ti concentration at these {0 0 1} defects suggests that they may be precursors for the various Ti-rich precipitates which have been identified in higher dose (4–100 dpa) studies of V–(4–5%)Cr–(4–5%)Ti at temperatures $\geqslant$ 400°C [11,31–34]. For example, Satou and coworkers [31] observed similar Ti- and Si-enriched platelet precipitates with a displacement vector of $a/3 \langle 0\ 0\ 1 \rangle$ on {0 0 1} habit planes in V–Cr–Ti–Si alloys following irradiation to 40 dpa at 520°C and 600°C.

5. Conclusions

Microstructural investigation of V–4Cr–4Ti specimens irradiated to relatively low fission neutron doses of 0.1–0.5 dpa has demonstrated that several complex radiation processes occur. The microstructure is independent of temperature between 110 and ~275°C, where it consists of a high density of small faulted dislocation loops. The high density and moderate barrier strength ($\alpha \leqslant 0.5$) of these dislocation loops produce significant radiation hardening with a concomitant sharp decrease in uniform elongation and an increase in the ductile to brittle transition temperature. Loop unfaulting occurred over a rather narrow temperature range centered near 300°C, and a high density of defect clusters on {0 0 1} habit planes was observed from 315°C up to the maximum irradiation temperature in this study of 505°C. The {0 0 1} defect clusters were enriched in Ti at elevated temperatures, and may be the precursors of the Ti-rich precipitates reported in higher dose studies at temperatures $\geqslant$ 400°C. It would be useful to investigate the microstructure of irradiated V–4Cr–4Ti at relatively low doses of 0.1–10 dpa to provide further insight into the microstructural evolution which occurs at temperatures above 400°C.

Acknowledgements

The authors thank L.L. Snead, W.S. Eatherly and J.L. Bailey for constructing, irradiating and disassembling the HFBR capsules. The assistance of Joe O'Connor, Guy Hartsough and Joel Errante in the research coordination group at HFBR was also of great value. This research was sponsored by the Office of Fusion Energy Sciences, US Department of Energy under contract DE-AC05-96OR22464 with Lockheed Martin Energy Research Corp., and was conducted utilizing the Shared Research Equipment (SHARE) program facilities at Oak Ridge National Laboratory.

References

[1] H. Matsui et al., J. Nucl. Mater. 233–237 (1996) 92.

[2] D.J. Alexander et al., 18th ASTM Symposium on Effects of Radiation on Materials, Hyannis, MA, in press; Fusion Materials Semiann. Prog. Report for Period ending June 30, 1996, DOE/ER-0313/20, Oak Ridge National Lab, 1996, p. 87.

[3] S.J. Zinkle et al., Fusion Materials Semiann. Prog. Report for Period ending December 31, 1996, DOE/ER-0313/21, Oak Ridge National Lab, 1996, p. 73.

[4] L.L. Snead, S.J. Zinkle, D.J. Alexander, A.F. Rowcliffe, W.S. Eatherly, presented at 8th Int. Conf. on Fusion Reactor Materials, Sendai, Japan, 1997; Fusion Materials Semiann. Prog. Report for period ending December 31 1997, DOE/ER-0313/23, p. 81.

[5] E.V. van Osch, these Proceedings.

[6] V.A. Kazakov, V.P. Chakin, Y.D. Goncharenko, these Proceedings.

[7] M. Satou, K. Abe, H. Kayano, J. Nucl. Mater. 233–237 (1996) 426.

[8] P.M. Rice, L.L. Snead, D.J. Alexander, S.J. Zinkle, Microstructure evolution during irradiation in: I.M. Robertson et al. (Eds.), DMRS Symp. Proc. Mater. Res. Soc., Pittsburgh, vol. 439, 1997, p. 343.

[9] J. Gazda, H.M. Chung, B.A. Loomis, M. Meshii, Microstructure evolution during irradiation, in: I.M. Robertson et al. (Eds.), MRS Symp. Proc. Mater. Res. Soc., Pittsburgh, vol. 439, 1997, p. 349.

[10] N. Doraiswamy, B. Kestel, D.E. Alexander, Microstructure evolution during irradiation, in: I.M. Robertson et al. (Eds.), MRS Symp. Proc., Mater. Res. Soc., Pittsburgh, vol. 439, 1997, p. 337.

[11] D.S. Gelles, P.M. Rice, S.J. Zinkle, H.M. Chung, these Proceedings.

[12] P.M. Rice, S.J. Zinkle, to be submitted.

[13] D.L. Smith, H.M. Chung, B.A. Loomis, H.-C. Tsai, J. Nucl. Mater. 233–237 (1996) 356.

[14] M. Iseki, Y. Kizuka, S. Mori, K. Kohmura, M. Kiritani, J. Nucl. Mater. 233–237 (1996) 492.

[15] H. Kawanishi, S. Ishino, E. Kuramoto, J. Nucl. Mater. 141–143 (1986) 899.

[16] H. Kawanishi, S. Ishino, J. Nucl. Mater. 155–157 (1988) 940.

[17] W.J. Phythian, B.L. Eyre, D.J. Bacon, J. Nucl. Mater. 155–157 (1988) 1274.

[18] B.L. Eyre, Fundamental aspects of radiation damage in metals, in: M.T. Robinson, F.W. Young Jr. (Eds.), CONF-751006-P2, National Tech. Inform. Service, Springfield, VA, vol. II, 1975, p. 729.

[19] D.J. Bacon, J.M. Harder, J. Nucl. Mater. 155–157 (1988) 1254.

[20] A.K. Seeger, 2nd UN Conference on Peaceful Uses of Atomic Energy, United Nations, New York, vol. 6, 1958, p. 250.

[21] U.F. Kocks, Metall. Trans. 1 (1970) 1121.

[22] K. Shiraishi, K. Fukaya, Y. Katano, J. Nucl. Mater. 44 (1972) 228.

[23] K. Shiraishi, K. Fukaya, Y. Katano, in: J.S. Watson, F.W. Wiffen (Eds.), Radiation Effects and Tritium Technology for Fusion Reactors, USERDA, vol. II, 1975, p. 122.

[24] R. Bajaj, M.S. Wechsler, Fundamental aspects of radiation damage in metals, in: M.T. Robinson, F.W. Young Jr. (Eds.), CONF-751006-P2, National Tech. Inform. Service, Springfield, VA, vol. II, 1975, p. 1010.

[25] E.R. Bradley, R.H. Jones, J. Nucl. Mater. 103 & 104 (1981) 901.

[26] H. Matsui, O. Yoshinari, K. Abe, J. Nucl. Mater. 141–143 (1986) 855.

[27] H. Takahashi, S. Ohnuki, H. Kinoshita, R. Nagasaki, K. Abe, J. Nucl. Mater. 155–157 (1988) 982.

[28] M.S. Wechsler, The Inhomogeneity of Plastic Deformation, Am. Society for Metals, Metals Park, OH, 1972, p. 19.

[29] R.J. Arsenault, J. Bressers, Metall. Trans. 8A (1977) 925.

[30] J. Gazda, M. Meshii, H.M. Chung, these Proceedings.

[31] M. Satou, K. Abe, H. Kayano, H. Takahashi, J. Nucl. Mater. 191–194 (1992) 956.

[32] H.M. Chung, B.A. Loomis, D.L. Smith, J. Nucl. Mater. 212–215 (1994) 804.

[33] M. Satou, K. Abe, H. Kayano, J. Nucl. Mater. 212–215 (1994) 794.

[34] K. Fukumoto, H.M. Chung, J. Gazda, D.L. Smith, H. Matsui, 18th International symposium on effects of radiation on materials, in: R.K. Nanstad et al. (Eds.), ASTM STP 1325, Amer. Soc. for Testing and Materials, Philadelphia, in press.